Investigating the functionality of a data acquisition system of a proton precession magnetometer

[1]DMMS Rathnasiri

[1]DMMS Rathnasiri
Department of Physics
University of Colombo
Colombo, Sri Lanka
2017s16303@stu.cmb.ac.lk
maleeshshehan@gmail.com
maleesh.shehan.dissanayake.mudiyanse
lage@cern.ch

***Abstract*— This experiment investigated an improved data acquisition system and its functionality to a proton precession magnetometer which has been previously developed at the Department of Physics, University of Colombo[1]. The proton precession magnetometer which is used to measure the geomagnetic field, can be recognized as a scalar magnetometer based on the concept of the nuclear magnetic resonance. The data acquisition system was introduced to improve the frequency measurement of the magnetometer which consisted of a magnetic sensor in dual solenoid configuration, and water as the proton rich material, and an instrumentation amplifier (AD8221). A PCM1808 module was introduced as an ADC to digitize the proton precession signal and transferred into an ESP32 module to store the data in a memory chip. Then the proton signal's frequency was determined with the aid of fast Fourier transform using Octave software. In order to examine the capability of the setup, the variations of the geomagnetic field were observed in a location in Kottawa, Sri Lanka and the mean geomagnetic field was determined with an accuracy of 0.12%.**

Keywords—proton precession magnetometer, nuclear magnetic resonance, geomagnetic field measurements

I. Introduction

Vector and scalar magnetometers are the two main classifications of magnetic sensors. Vector magnetometers are found to measure the magnetic field components with respect to their relative direction, and the absolute magnitude of the magnetic fields is measured irrespective of their direction, in a scalar magnetometer. The scalar magnetometers are based on the magnetic resonance which can be further extended to Nuclear Magnetic Resonance (NMR) and Electron Spin Resonance (ESR). As common scalar magnetometers, Proton Precession Magnetometer (PPM), and Overhauser Magnetometer (OVM) can be recognized.[2] In this particular study, the Proton Precession Magnetometer (PPM) is the main focus.

Particularly, a Proton Precession Magnetometer can be regarded as a widely used magnetometer based on the Nuclear Magnetic Resonance, which has variety of usages in geophysics applications and earth magnetic field measurements.[3]

II. Principle of Operation

The precession of protons in a magnetic field is the basic idea in the proton precession magnetometer. It measures the proton precession signal to determine the geomagnetic field. Therefore, it is needed to polarize the protons beforehand in order to have a precession and then the precession should be measured.

First, the protons in a sample are magnetically polarized with the aid of an applied magnetic field where it leads to a phase coherence. In this study, hydrogen nuclei contained in a sample of distilled water was chosen, and the external magnetic field was produced by a current in a coil of wire positioned around the water sample.

According to quantum physics, it is known that when a proton is spinning, a magnetic moment is produced due to the spin, and it is determined that the magnetic moment (μ) is proportional to its spin momentum (L) as expressed in the equation (1). [4]

$$\mu = \gamma L \tag{1}$$

γ is known as the gyromagnetic ratio which is found to be equal to a constant value of 2.6751987×10^8 s^{-1} T^{-1}.

After that, the polarizing current is turned off so that there will be no magnetic field applied to the protons and it is determined that the protons will tend to have a precession motion which is commonly known as the Larmor precession.

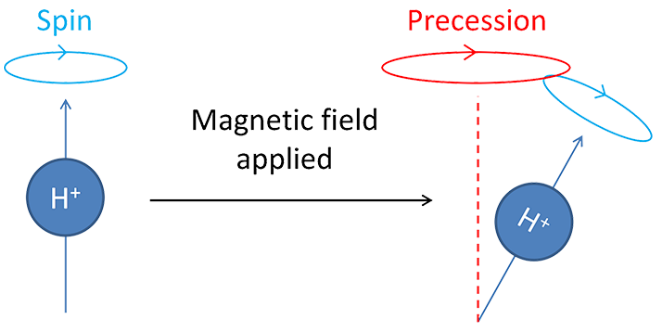

Figure II-1 When the polarizing current is turned off the protons tend to have a precession motion which is commonly known as the Larmor precession (Image Source: https://www.radiologycafe.com/images/physics/mri-intro-precession@2x.png)

It is found that a signal is induced inside the coil with an angular frequency known as the precession frequency of the Larmor signal (ω) which tends to be proportional to the applied external magnetic field (B) as shown in the equation (2). (γ is known as the gyromagnetic ratio as mentioned earlier). [4]

$$\omega = \gamma B \tag{2}$$

It is also known that the amplitude of the induced sinusoidal voltage decreases exponentially, when the protons return to their original state. Therefore, the measurements have to be taken quickly before the protons coming to the random orientation. [5]

After determining the Larmor frequency it is known that the geomagnetic field can calculated using the Larmor relationship as shown in the equation (3) where the Larmor frequency is represented by ω and B and m_p represent the magnetic field and the mass of a proton respectively.

$$\omega = \frac{eg_p}{2m_p} B \tag{3}$$

This equation can be rearranged to determine the magnetic field B, by substituting the relevant values, in the equation (4) where the magnetic field B is calculated in nT (nano Tesla) and f is measured in Hz. [1]

$$B = 23.496241\, f \tag{4}$$

The precession frequency corresponding the earth magnetic field happens to be in audio frequency region.

III. MAGNETOMETER CONSTRUCTION

The schematic diagram of the proton precession magnetometer can be seen in the figure III-1.

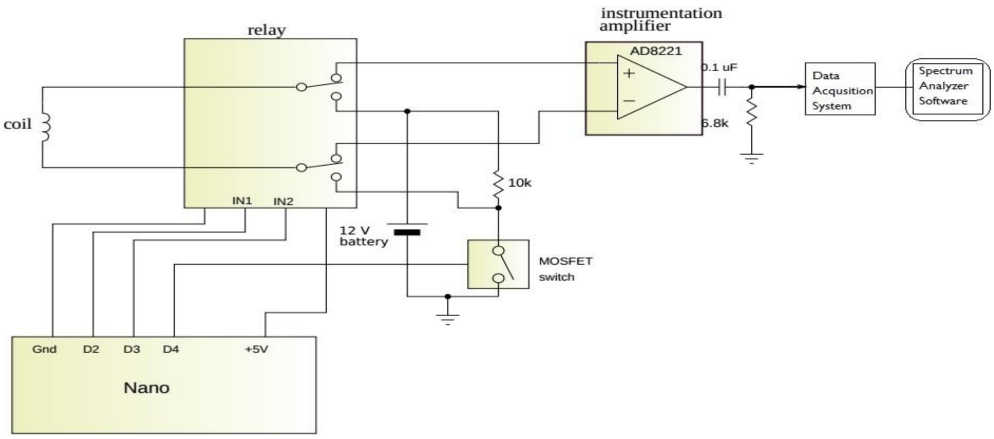

Figure III-1 The schematic diagram of the proton precession magnetometer.

The data acquisition system was used to improve the frequency measurement, whereas a combination of a PCM 1808 ADC and an ESP 32 was used in making.

The Arduino nano module was used to switch the coil between the 12 V battery and the instrumentation amplifier. After powering the coil for 5 seconds by the battery, the oil is allowed to discharge for about 10 ms and then connected to the amplifier for another 5 second period.

PCM1808 is a high performance and low cost, stereo 24-bit analog to digital converter, which is capable of taking data at sampling speeds up to about 96 kHz. It transfers data to ESP32 via I2S protocol. The high ADC resolution of this device eliminates the need for signal amplification after the instrumentation amplifier.

The ESP32 was selected due to its support for I2S communication. While there are many ESP32 based modules, only a few of them expose the GPIO0 pin which is needed for generating the I2S clock signal for the PCM1808.

The camera module of the ESP32 CAM module was removed during this application. Because the ESP32 CAM has a very limited number of IO pins, and because some of the pins used for SD card interfacing was needed for controlling the PCM1808, the data storage capability in the SD card could not be used. Instead, the plan was to transfer data to a PC through Wi-Fi.

IV. INVESTIGATION OF THE DATA ACQUISITION SYSTEM

A. *Using the ESP32-CAM module in the DAQ System*

Initially, this section of the circuit was tested, where the ESP32-CAM module was used along the PM1808 as shown in the figure IV-1.

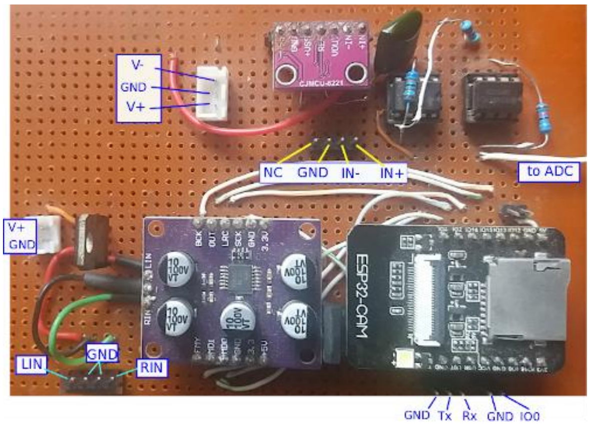

Figure IV-1The initially introduced DAQ system consisted of an ESP32-CAM module with a PM1808 ADC

The attempt to transfer data through Wi-Fi was not successful due to relatively weak Wi-Fi communication of the ESP32-CAM.Therefore, an alternative method had to be used for the development of the DAQ system.

B. *Using the ESP32-WROOM module in the DAQ system*

Then as an alternative to the previous module, the ESP32-WROOM module was introduced along with the PCM1808 ADC as shown in the figure IV-2.

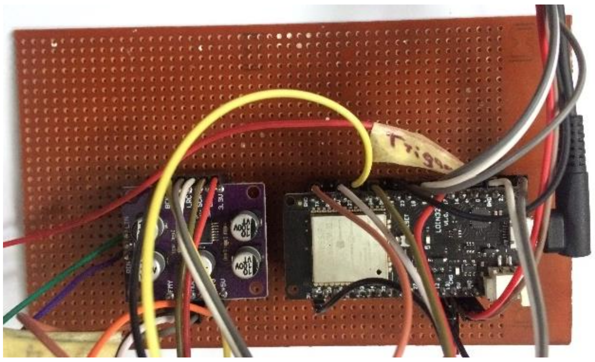

Figure IV-2 The secondly introduced DAQ system consisted of an ESP32-WROOM module with a PM1808 ADC

ESP32 WROOM is another ESP32 based module that exposes GPIO0 pin. With more available IO pins, it was possible to interface an SD card to store collected data in the SD card. A few data sets were obtained using this section of the circuit with the input pin of the PCM 1808 left open, and then the voltage values were Fourier analyzed to find its constituent frequency components. Then the code was developed to determine the average Fourier spectrum over the obtained data sets automatically and the resulting spectra plotted over few data sets as shown in the figure IV-3 and IV-4.

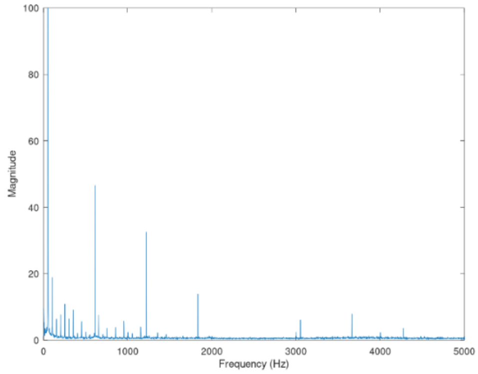

Figure IV-3 Fourier spectrum obtained for 4 data sets. The peaks in this spectrum must be due to noise picked up by the input pin of the PCM1808.

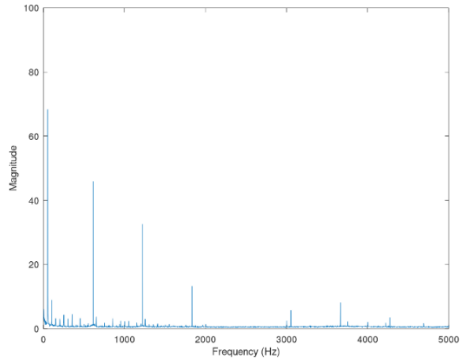

Figure IV-4 Fourier spectrum obtained for 10 data sets. It shows the idea that Fourier sampling for a higher number of data sets is always recommended.

It was clear that when the average Fourier spectrum was obtained for a larger number of data sets, the unwanted noise signals were diminished considerably.

C. *Testing the complete circuit*

After investigating the PCM1808 with the ESP32-WROOM, the next idea was to integrate the already tested components with the other components of the circuit as shown in the schematic diagram in the figure IV-5.

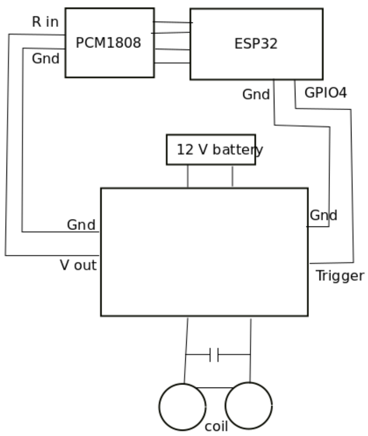

Figure IV-5 The block diagram for the complete circuit

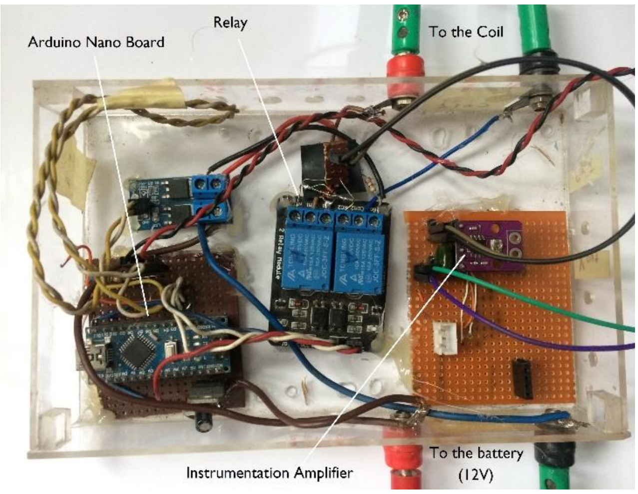

Figure IV-6 The complete circuit accessories consisting the relay to control the polarization, the nano board which controls the relay and the instrumentation amplifier. A 12V battery was used to power up the coil where few batteries were used to power up the instrumentation amplifier.

Figure IV-7 The solenoidal coils used as the magnetic sensor. They are found to be easy to wind and with high internal magnetic field uniformity. Dual solenoid configuration is used to reduce the noise.

Then few measurements were taken, and after analyzing the data the ADC values showed the following behavior shown in the figure IV-9.

With respect to the ADC value's behavior in the figure IV-9, it was understood that, for each data set, a considerable amount of data for a set had to be discarded due to the fact that sometimes, the PCM1808 starts taking data before the instrumentation amplifier input is connected to the coil. This happens because the switching is done by a mechanical relay

Therefore, as a solution, the code was developed to take more data using the setup so that some initial portion of a particular data set can be discarded to avoid the previously explained situation. The first 1000 data values were discarded and the ADC values and the Fourier spectra were plotted using the measurements. But however, the improvised technique was found to be not successful to measure the magnetic field. Therefore, the setup was further developed to take accurate measurements.

Following that, after making some additional hardware and software development to the system. The introduced data acquisition system was found to be functional.

V. Signal Analysis

As it was explained earlier, the geomagnetic field was calculated using the Larmor relationship as shown in the equation (4).

$$B = 23.496241\, f \tag{4}$$

In this case, the magnetic field B is calculated in nT (nano Tesla) where f is the frequency of the proton precession signal measured in Hz.

A. Initial Investigation

The primary inspection was conducted at a location in Kottawa, Sri Lanka. A peak around 1752 Hz was observed in the Fourier spectrum after the analysis as shown in the figure IV-8. It corresponded to a geo magnetic field of 41165 nT with an uncertainty of ±23nT. The authenticity of the revealed FFT peak was confirmed by positioning a metal

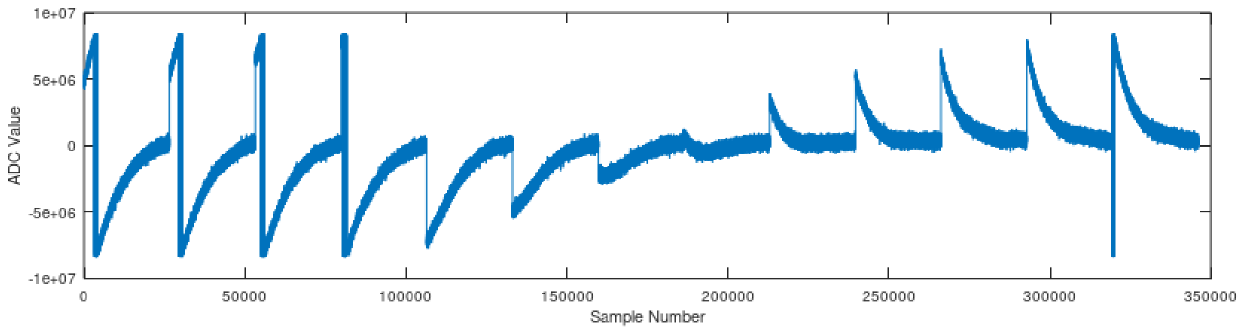

Figure IV-8 The plot of the ADC value vs the sample number. The faulty samples can be easily detected using this graph. As shown in the figure a considerable amount of data for a set had to be discarded due to the fact that the coil needed some time to discharge before being connected to the instrumentation amplifier.

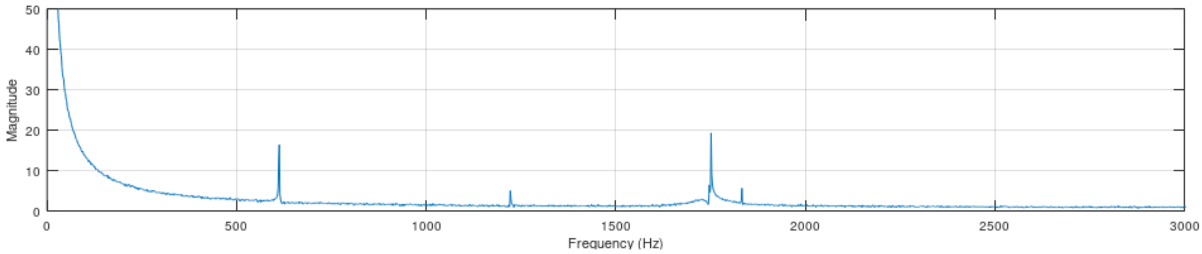

Figure V-2 The Fourier spectrum of the initial investigation. A peak around 1752 Hz was observed It corresponded to a geo magnetic field of 41165 nT with an uncertainty of ±23nT.

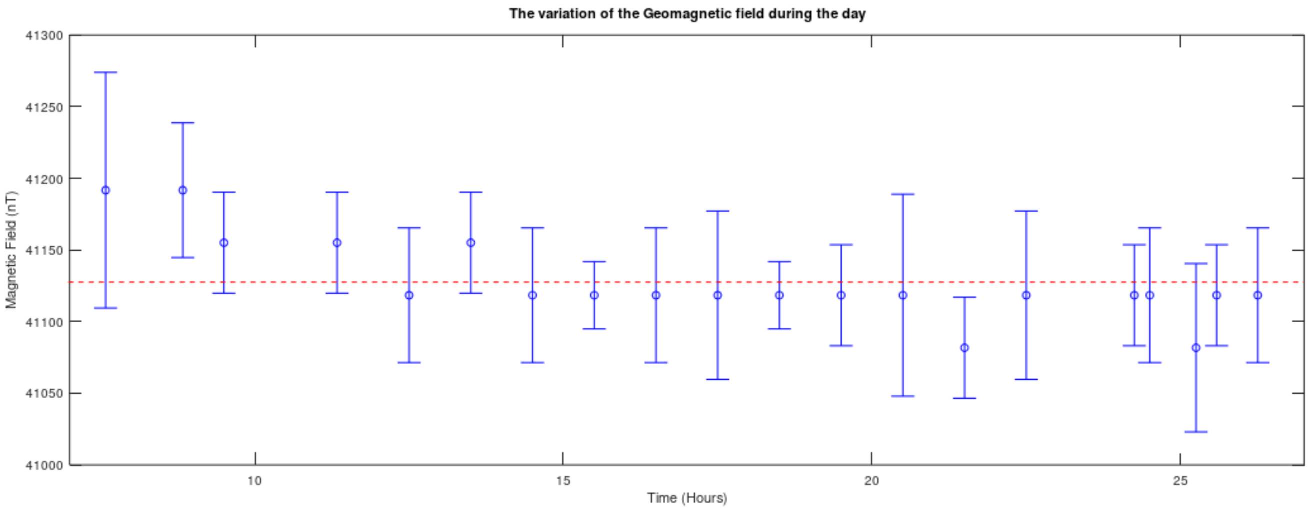

Figure V-1 The variation of the Geomagnetic Field during 0730h (GMT) on 25.07.2021 to 0230h (GMT) on 26.07.2021 at Kottawa, Sri Lanka. The mean magnetic field (shown in the dotted red line) was determined as 41128 nT with an uncertainty of ±48 nT.

object close to the magnetic sensor which caused the signal to disappear.

B. Daily Variation of the Geomagnetic field

The data were obtained for 19 hours from 0730h (GMT) on 25.07.2021 to 0230h (GMT) on 26.07.2021 at Kottawa, Sri Lanka to observe the daily variation of the geomagnetic field. The resulting graph is shown in the figure V-I.

The mean magnetic field during the respective day was determined as 41128 nT with an uncertainty of ±48 nT which was found be consistent with the computed value by the National Centers for Environmental Information (NOAA). [6]

VI. Conclusions

Previously described results confirm that the introduced data acquisition system which consisted the PCM 1808 Analog-to-Digital Converter and the ESP32-WROOM module is proficient in measuring the geomagnetic field and its variation during the day precisely.

Acknowledgment

I am really thankful to my supervisor Dr. MK Jayananda, for his immense support while taking his valuable time for the useful and detailed discussions which hugely helped me to complete this project successfully. Similarly, I gratefully express my gratitude to the Department of Physics, University of Colombo.

References

[1] W. D. S. Ruhunusiri and M. K. Jayananda, “Construction of a Proton Magnetometer,” *Proc. Tech. Sess. Inst. Phys. - Sri Lanka*, vol. 24, pp. 78–85, 2008.

[2] P. R. (ed), “Magnetic Sensors and Magnetometers,” *Meas. Sci. Technol.*, vol. 13, no. 4, pp. 645–645, Apr. 2002, doi: 10.1088/0957-0233/13/4/707.

[3] P. Mahavarkar, S. Singh, S. Labde, V. Dongre, and A. Patil, “The low cost Proton Precession Magnetometer developed at the Indian Institute of Geomagnetism,” *J. Instrum.*, vol. 12, no. 5, 2017, doi: 10.1088/1748-0221/12/05/T05002.

[4] W. Luo *et al.*, “Research on an omnidirectional proton precession magnetometer sensor based on solenoidal coils,” *I2MTC 2019 - 2019 IEEE Int. Instrum. Meas. Technol. Conf. Proc.*, vol. 2019-May, pp. 1–6, 2019, doi: 10.1109/I2MTC.2019.8827001.

[5] F. Mahboubian, H. Sardari, S. Sadeghi, and F. Sarreshtedari, “Design and Implementation of a Low Noise Earth Field Proton Precession Magnetometer,” *ICEE 2019 - 27th Iran. Conf. Electr. Eng.*, pp. 345–347, 2019, doi: 10.1109/IranianCEE.2019.8786372.

[6] Ngdc.noaa.gov. 2021. NCEI Geomagnetic Calculators. [online] Available at: <https://www.ngdc.noaa.gov/geomag/calculators/magcalc.shtml?#igrfwmm> [Accessed 26 July 2021].